RELATION BETWEEN MECHANICAL PROPERTIES AND PYROLYSIS TEMPERATURE OF PHENOL FORMALDEHYDE RESIN FOR GAS SEPARATION MEMBRANES

#MONIKA ŠUPOVÁ*, JAROSLAVA SVÍTILOVÁ*, ZDENĚK CHLUP**, MARTIN ČERNÝ*, ZUZANA WEISHAUPTOVÁ*, TOMÁŠ SUCHÝ*,***, VLADIMÍR MACHOVIČ*,****, ZBYNĚK SUCHARDA*, MARGIT ŽALOUDKOVÁ*

*Institute of Rock Structure and Mechanics, Academy of Sciences of the Czech Republic (ASCR), V Holešovičkách 41, 182 09 Prague, Czech Republic
**Institute of Physics of Materials, ASCR, v.v.i., Žižkova 22, 616 62 Brno, Czech Republic
*** Laboratory of Biomechanics, Czech Technical University, Faculty of Mechanical Engineering, Department of Mechanics, Biomechanics and Mechatronics, Technická 4, 166 07 Prague, Czech Republic
****Institute of Chemical Technology Prague, Technická 5, 166 28 Prague 6, Czech Republic

#E-mail: supova@irsm.cas.cz

Submitted November 11, 2011; accepted January 24, 2012

Keywords: Glassy carbon, Membranes, Mechanical properties, Phenol-formaldehyde resin, Pyrolysis

The aim of this paper has been to characterize the relation between the pyrolysis temperature of phenol-formaldehyde resin, the development of a porous structure, and the mechanical properties for the application of semipermeable membranes for gas separation. No previous study has dealt with this problem in its entirety. Phenol-formaldehyde resin showed an increasing trend toward micropore porosity in the temperature range from 500 till 1000°C, together with closure of mesopores and macropores. Samples cured and pyrolyzed at 1000°C pronounced hysteresis of desorption branch. The ultimate bending strength was measured using a four-point arrangement that is more suitable for measuring of brittle materials. The chevron notch technique was used for determination the fracture toughness. The results for mechanical properties indicated that phenol-formaldehyde resin pyrolyzates behaved similarly to ceramic materials. The data obtained for the material can be used for calculating the technical design of gas separation membranes.

INTRODUCTION

There are many possible applications for carbons obtained from phenol formaldehyde (PF) resins. Some of these, e.g. precursors for molecular sieves or membranes, have been reported in the literature [1-4]. Polymeric membranes have been developed for a variety of industrial applications. Carbon membranes have several properties superior to those of polymeric membranes. They display a superior permeabilities-selectivity combination, do not have compaction and swelling problems, and can operate in the presence of organic vapour, non-oxidizing acid or alkaline environments. They are suitable for use in separation processes in the range 500-900°C. Carbon membranes are mechanically much stronger, and can withstand higher pressure differences for a given thickness. However, they require purification to remove adsorbed traces, and they demonstrate a high selectivity for certain gas mixtures. They are only suitable for gases with molecular sizes smaller than 0.4-0.45 nm [4]. In addition, carbon membranes are very brittle and fragile, and for practical applications they therefore need to be deposited on a suitable support [5, 6]

When phenolic resin is heated in an inert atmosphere to temperatures exceeding 300°C, there are high yields of disordered non-graphitizing carbon with glass-like properties. In the transition process from resin to glassy carbon, pores develop due to the pyrolysis gases that are produced. Consequently, the microstructure of carbonized products is very porous. According to the standard nomenclature [7], pores are classified as micropores (d < 2 nm), mesopores (d = 2-50 nm), macropores (d = 50-15 000 nm), and coarse pores (d > 15 000 nm). Porous structure is affected by the rate of gas evolution and the rate of diffusion of the evolved gases, which are closely related to the carbonization conditions, e.g. heating rate and sample dimension. The weight loss is significant between 300°C and 600°C [8-10]. Fott et al. [11] found that the porosity of the micropores increased with the carbonization temperature, and reached a maximum at a temperature of 750°C. With a further increase in temperature, closure of the microporous structure took place. These investigations correlate with the results of some other authors [12,13]. Centeno and Fuertes [14] observed that the carbonization temperature has a marked influence on the characteristics of carbon molecular sieve membranes. The He permeability of the membrane

increased with increasing heat treatment temperature in the range 500-700°C. The carbon membrane obtained at 700°C showed He permeability 30 times higher than the He permeability observed for cured phenolic resin. Another factor that has a major influence on the porosity development and the structural changes of the resulting carbon spheres is the carbonization atmospheres. Kim et al. [15] found that in comparison with an N_2 atmosphere, a CO_2 atmosphere resulted in more surface pits, a greater surface area and a larger micropore volume of the carbon spheres. In addition, in a CO_2 atmosphere, a larger carbon layer and higher contents of reactive edge carbon atoms in the carbon layers were facilitated. Lenghaus et al. [16] found that under the same carbonisation conditions, *para* alkyl phenols produced carbons with broad micropores, while phenol and 3,5-dimethylphenol produced carbons with narrow micropores. Carbonised materials based on *para* alkyl phenols had an unusually high degree of microporosity in comparison with conventional phenol formaldehyde resins. Many methods [17,18] have been proposed for controlling mesopores, e.g. catalytic activation [19-21], polymer blend carbonization [22, 23], polymer deposition [24,25] and template carbonization [26,27].

The microstructure formed during carbonization has a significant influence on the mechanical properties of the products. Laušević and Marinković [28] showed that the flexural strength and flexural modulus decreased with increasing temperature, reaching a minimum at approximately 500°C, and then suddenly increased. Different samples exhibited slightly different strengths, but no variation in the modulus was observed for different samples, indicating that the strength is much more sensitive to inherent faults in the structure of the samples. When the heating rate is faster than 30°C/hr, the flexural modulus decreases drastically, owing to the high porosity of the carbonized samples [29]. By contrast, the pore structure formed at lower heating rates is observed to be uniform, and consists mainly of narrow pores less than 0.1 μm in radius. Choe et al. [29] determined the relation between critical heating rate (H_{ci}) and sample dimension (thickness). In the case of H_{ci}, the rate of gas evolution is much higher than the rate of diffusion, and as a result the flexural modulus suddenly drops. H_{ci} falls off exponentially with increasing sample thickness. Another variable processing parameter - soaking time duration, was studied by Glogar and Balík [30].

Our paper focuses on the relation between the pyrolysis temperature of phenol formaldehyde resin, the development of a porous structure, and the mechanical properties for the application of semi-permeable membranes for gas separation. Mechanical properties such as mechanical strength, hardness, fracture and elastic behaviour will be discussed in detail. This problem has not previously been studied in its entirety, though gas transport and separation characteristics have already been investigated in detail by many researchers.

EXPERIMENTAL

Bodies of resite in the form of plates approximate 1.2 mm in thickness were prepared by the interaction of formaldehyde with phenol in a molar ratio of 1.02 under alkaline conditions (NH_4OH) at 95°C for 30 minutes. The water was removed by distillation under reduced pressure at 55°C. Then the mixture was diluted by ethanol and spread on the mould. The ethanol was removed by heating at 40°C for 200 hours. The gelified polymer was taken out of the mould and cut into circular membranes and polymerized at 60°C for 4 hours. The samples were cured in two steps: at 90°C (4 hours) and at 127°C (4 hours), followed by a post-curing process at 150°C for 4 hours. The curing process was proposed according to the results of a dielectric analysis (ECOSOFT, CZ). Measurements of dielectric properties can be used to monitoring of chemical reactions in organic materials. The change in resistance of studied polymer is related to its change of viscosity. More details about this method are described in paper [31]. Carbonization was carried out up to 1000°C in nitrogen at a flow rate of 40 cm^3/min with heating rate 10°C/hr and soaking time duration 10 hours, which correlates with published data, taking sample thickness and soaking time duration into account [29,30]. A controlled cooling rate of 20°C/hr was maintained down to room temperature.

The pyrolyzed samples were investigated by measu-ring their weight, dimensions and bulk density. The total cumulative volume V_{mmc} of mesopores (V_{meso}), macro-pores (V_{macro}), and coarse pores (V_{coarse}) and their pore size distribution were determined with sampkle piece 5 mm in size, using coupled Pascal 140 + 240 porosimeters by Thermo Electron - Porotec. The samples were evacuated at 353 K for 2 h prior to analysis, and were then evacuated in the instrument until a stable pressure was reached. A contact angle of 140° and a value of 480 $.10^{-3}$ $N.m^{-1}$ for the Hg/air interfacial tension were used in the Washburn equation to determine the pore size distribution [32]. Each sample was measured twice, and the coefficients of variation for measurement of cumulative volume V_{mmc} were less than 7 %. In order to determine the micropore volume V_{micro}, CO_2 isotherms were measured using a Hiden IGA 002 gravimetric sorption analyzer. For CO_2 sorption, the samples were prepared with grain sizes < 0.2 mm, and the sample weight was about 0.3 g. Before measurement, the samples were degassed at a temperature of 80°C under vacuum 10^{-6} Pa up to constant weight. The measurements were performed at a temperature of 25°C up to pressure 0.1 MPa. The coefficients of variation for measurement of adsorbed amounts of CO_2 (g/g) on carbonaceous materials are less than 1%.

Some of the samples were investigated by scanning electron microscopy analysis, using a Quanta 450 electron SEM microscope (FEI Company, USA), under

a high vacuum, with an Au coating film on the samples.

Fourier transform infrared spectra of cured samples (PF 150) and pyrolyzed samples (PF 500) were taken with Protégé 460 E.S.P. (Thermo-Nicolet, Inc., USA) over the range between 4000 and 400 cm^{-1} at resolution 4 cm^{-1}, averaging 128 scans, using the ATR technique. Due to the high content of carbon phase in other pyrolyzed samples (PF 600, 700, 800, 1000), the structure was characterized with the help of Raman spectroscopy. The Raman spectra were measured using a Labram HR Raman dispersive spectrometer (Jobin Yvon). The parameters from three different areas (diameter ca 1 μm) were averaged. The spectra were separated into four bands at approx. 1150, 1340, 1550 and 1600 cm^{-1}, and were fitted using the mixed Gaussian–Lorentz function.

The static Young's modulus and ultimate strength in bending of the cured sample (150°C) and samples carbonized at different temperatures (500, 600, 700, 800, 1000°C) were determined using an Inspekt 100 (Hegewald & Peschke) testing machine at a cross-head speed of 0.5 mm/min in the four-point bending arrangement (span length 40 mm). A three-point bending test and a fracture toughness test were performed using the Zwick Z50 (Zwick, Ulm, Germany) electro-mechanical testing system (span length 10 mm). The fracture toughness values were calculated from the established maximum force and from the compliance function calculated on the basis of the Bluhm slice model [33]. The dynamic Young's modulus was measured by a resonant frequency method using an Erudite tester (C.N.S. Electronics). The response of the material to mechanical loading was determined using a fully-instrumented indentation test with depth measurement resolution of 20 nm. A Zwick Z2.5 testing machine equipped with a microhardness head ZHU0.2 (200 N load cell) with optics was employed. All of the indentation experiments were performed at the same peak load of 2 and 5 N and in accordance with the standard for the Vickers hardness test [34]. All prepared indents in the microhardness test were observed using a LEXT OLS3100 optical and laser confocal microcope (Olympus, Japan). The chevron notch technique was used to determine the fracture toughness. More details about this technique are described in papers [35,36]. We used samples with nominal dimensions 1.5×2.5×15 mm^3 equipped with a chevron notch cut with an Isomet 5000 precise diamond saw (Buhler, USA).

A statistical analysis for all mechanical properties tests was carried out using STATGRAPHICS Centurion XV and also StatPoint, USA. Outlier identification was performed via the Grubbs and Dixon tests. Tests for normality were performed via the Chi-Squared, Shapiro-Wilk test. Homoscedasticity was checked for the application of ANOVA parametric tests (the Leven, Bartlett and Cochran tests were used). The statistically significant differences were checked by nonparametric methods. The Kruskal-Wallis test was used for this purpose. The Mann-Whitney test was used as a post-hoc test. The confidence intervals for the mean values were calculated at a significance level of a = 0.05.

RESULTS AND DISCUSSION

Structure characterization

Table 1 presents the weight loss, linear shrinkage and variation in bulk density during carbonization. The results indicate that the process of carbonization is almost completed at 800°C. The most significant weight loss (40%) is up to 600°C, while in the high temperature treatment (HTT) range from 700-1000°C the weight loss is about 3%. The bulk density decreased with increasing pyrolysis temperature, and reached the minimum value of 1.17 g/cm^3 at 500°C. Above this temperature, the bulk density increased till the highest value of 1.47 g/cm^3 at 800°C, and then remained almost constant. The same trend was observed by Fott et al. [11] and by Choe et al. [29] and it has been explained by pore formation, volume contraction and chemical densification resulting from a change in the chemical structure of the resin.

PF resin for membrane application is usable in the form of its pyrolyzates prepared at temperatures above 500°C. The porosity, structure characteristics and mechanical properties are therefore discussed in detail for the temperature range 500-1000°C, and are

Table 1. Description and physical properties of the investigated PF resin samples.

Sample notation	Notes	Linear shrinkage (%)	Weight loss (%)	Bulk density (g/cm^3)
PF 150	Cured at 150°C	0	0	1.18
PF 300	Pyrolyzed at 300°C	1	4	1.18
PF 400	Pyrolyzed at 400°C	5	5	1.18
PF 500	Pyrolyzed at 500°C	13	37	1.17
PF 600	Pyrolyzed at 600°C	17	40	1.25
PF 700	Pyrolyzed at 700°C	20	40	1.37
PF 800	Pyrolyzed at 800°C	22	42	1.47
PF 1000	Pyrolyzed at 1000°C	23	43	1.45

confronted with the properties of resite (PF 150).

The "fingerprint" regions of the FTIR spectra of samples PF 150 and PF 500 are shown in Figure 1. In the spectrum of PF 150, the band 1650 cm^{-1} as a weak shoulder on the 1600 cm^{-1} doublet (aromatic ring stretching) can be ascribed to carbonyl groups (benzophenones) produced through primary oxidative degradation [37, 38].

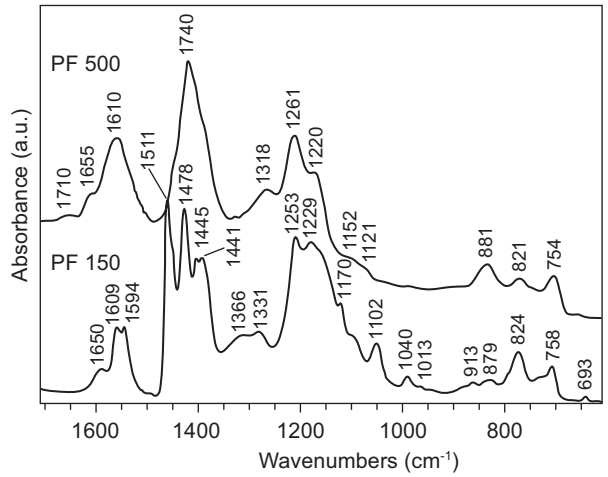

Figure 1. ATR FTIR spectra of a cured sample (PF 150) and a pyrolyzed sample (PF 500).

Ethers are formed as a consequence of the condensation reaction. Evidence of this is found in the band at 1253 cm^{-1}. The absorption at 1229 cm^{-1} is due to phenolic OH and CO stretching. Band 1366 cm^{-1} belongs to the OH band and is weak in intensity due to condensation processes and crosslinking [37]. Peaks 1013 and 1331 cm^{-1} are bands of the CH_3 group attached to the aromatic ring [37]. The bands of the methylene group are at 913, 1441 cm^{-1}. However, the band at 1441 cm^{-1} is especially significant because of the formation of methylene links during the curing process [39]. The peak at 1170 cm^{-1} corresponds to the 2- and/or 4-substituted ring, while the absorbance of the peaks at 1511, 1455, 1102, 824 and 758 cm^{-1} belongs to the 1,2,4-trisubstituted ring. Indications of changes in substitutions on the benzene ring can also be found in the band at 879 and 1476 cm^{-1}, indicating a tetra-substituted ring. Peak 693 cm^{-1} belonging to the monosubstituted ring is very weak, because of the higher substituted ring formation in the curing process. In the FTIR spectrum of sample PF 500, all the bands become more complex, showing that the main structure of the polymer is still there, but it is changing toward a polyaromatic structure. This can be seen by observing the 1600 cm^{-1} band, which was originally a sharp doublet but becomes a broad band covering a range of

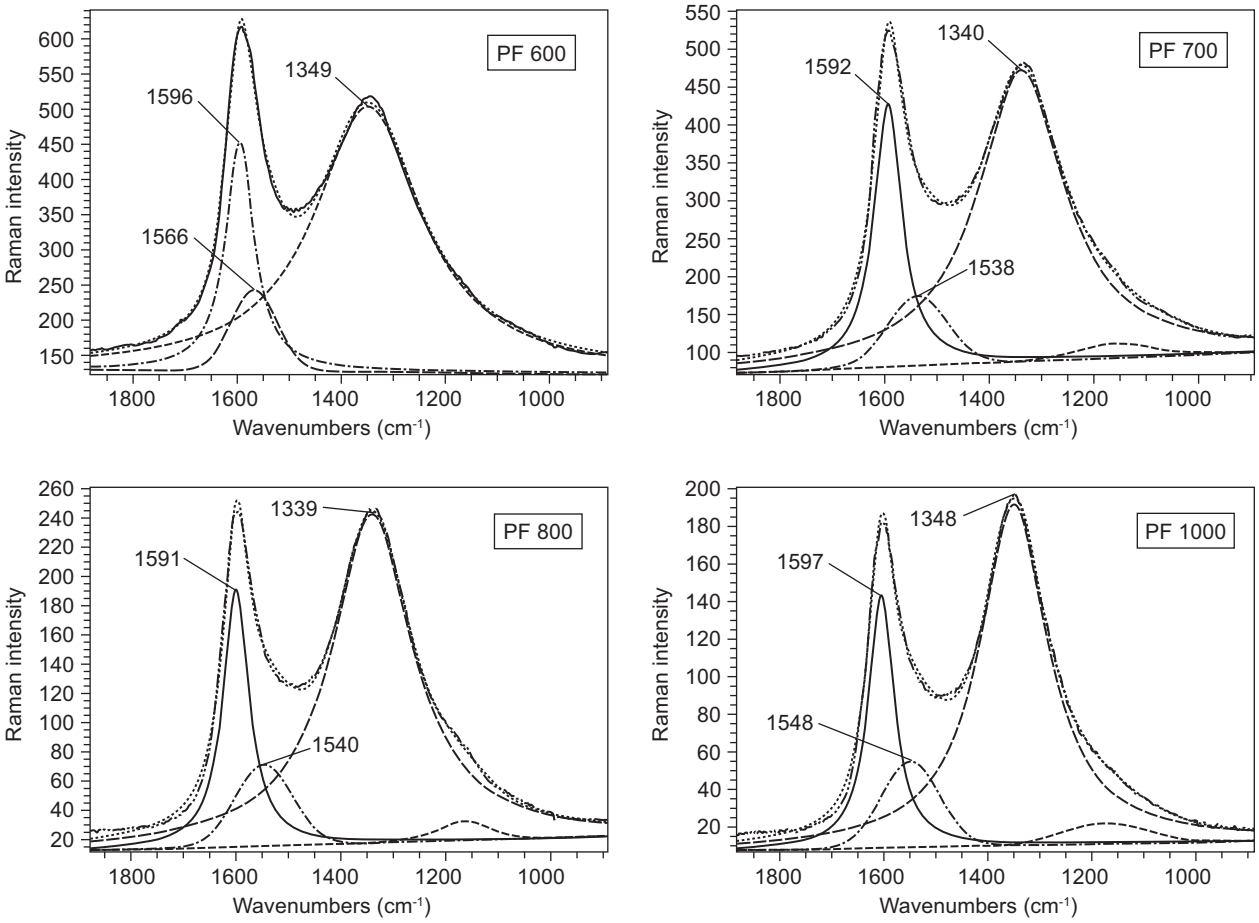

Figure 2. Separated Raman spectra of pyrolyzed samples

ca 100 cm^{-1}, typical for a polyaromatic system [39]. The band typical for a benzophenone structure (1654 cm^{-1}) is still present. Bands 1470 and 881 cm^{-1} (tetra-substituted ring) become more intensive than the bands of the trisubstituted ring. The tri-substituted ring is changed to a tetra-substituted ring during the degradation process. The band at ca 1260 cm^{-1} (an ether band) also increased in intensity, due to oxidation. Evidence of oxidation is given by the new weak absorption growing at 1710-1740 cm^{-1} due to carboxylic acid formation during the PF resin degradation process [38]. Up to 500°C, however, the polymer network remains essentially unaffected, whereas above 500°C dramatic changes were observed in the IR spectra. The network collapsed with the formation of polyaromatic domains [37, 40]. Evelyn et al. [41] proved using Raman spectroscopy that the greatest carbonization occurred at 500-600°C. The structures of other samples (PF 600-PF 1000) were therefore characterized using Raman spectroscopy. The separated Raman spectra are shown in Figure 2.

Two major characteristic bands can be found in the Raman spectra of these carbon-rich materials. First, the graphite band (G-band), located at 1575 cm^{-1}, is the fundamental Raman mode of sp^2 binding structures caused by the stretching vibrations of the C–C bonds. In the case of carbon materials with a random carbon structure (so-called disordered carbon), the band maximum shifts toward 1580–1610 cm^{-1}, and its half-width increases. Second, a disordered band (D-band), usually lying between 1300 and 1400 cm^{-1}, can be found in amorphous materials. Another band that appears in the spectra of carbon-rich materials is a wide band at ~1550 cm^{-1} belonging to the amorphous graphitic phase and, as follows from Table 2, the area of this band increased slightly with pyrolysis temperature. By contrast, the area ratio ($A_{D(1350)}/A_{G(1590)}$) decreased slightly. However, the same trend was not observed for the intensity (I_D/I_G) ratio. As shown in Figure 2 and in Table 2, the intensity of the D-band increased with temperature. This is an indication of greater disorder, corresponding to an increase in polymeric disordered carbon. This indicates that more edges have been created in the aromatic sheets. The same trend was observed by Evelyn et al. [41]. Parameter f (the fractional value for the amount of disordered carbon), which is related to the intensity of bands D and G according to equation 1 [42]:

$$f = \frac{I_D}{I_D + I_G} \quad (1)$$

also proved the increasing tendency of I_D and consequently the amount of disordered polymeric carbon. The half-width of bands D and G decreased with increasing temperature. The extreme width of these bands at lower temperatures was observed by Kishore et al. [42]. They explained this by two possible situations. Firstly, the material exists in several different spectroscopic states differing only marginally from each other. Secondly, a stable single-phase material consists of small domains distributed over a size range. The most drastic changes in the structure of phenol formaldehyde resin occur in the range 500-600°C. With further increasing pyrolysis temperature, the amount of disordered polymeric carbon grows. Although the literature suggests full carbonization at 1000°C and a pure form of polymeric carbon, Evelyn et al. [41] proved by Rutherford backscattering spectrometry (RBS) that at 1000°C there are still significant amounts of oxygen and other impurities. This material shows different behaviour from graphitic or graphitizable materials.

The results presented in Figure 3 show an increasing trend in the porosity of micropores in the temperature range from 500 till 1000°C. By contrast, with increasing temperature (in this temperature range) mesopores and macropores increasingly close. In the temperature range 600-1000°C, the relative volume of coarse pores predominates over the volumes of mesopores and macropores, as is very clear from the pore size distribution shown in Figure 4. Coarse pore formation is usually

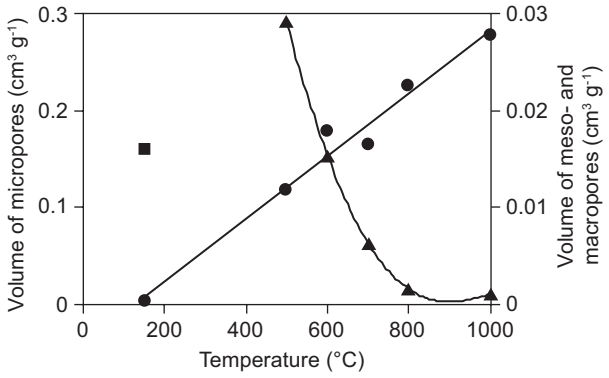

Figure 3. Dependence of the pore types on temperature of pyrolysis. ● Micropores, ▲ Meso- and Macropores, ■ Meso- and Macropores - Resite

Table 2. Structural parameters of the pyrolyzed samples.

Sample	$FWHM_D$	$FWHM_G$	A_G/A_{1550}	A_D/A_G	I_D/I_G	f (%)
PF 600	223	66	2.84	4.00	0.78	46
PF 700	200	63	2.81	3.89	0.88	47
PF 800	184	61	2.33	3.87	0.98	50
PF 1000	170	60	1.90	3.83	1.06	51

caused by exceeding the critical heating rate [29]. Although the optimal heating rate was used in this work, coarse pores appeared. During carbonization of the polymers, thermal degradation takes place with simultaneous action of mechanical stress. Under these conditions, microdefects may easily occur even during the carbonization process [43]. The volume of coarse pores reached the maximum at 800°C. It can influence the mechanical properties, as will be discussed below. The occurrence of coarse pores in the form of a surface crack was proved by SEM (Figure 5). In resite sample PF 150, mesopores prevail over other pore types. During carbonization, mesopores may serve to remove the pyrolysis gases. The maximum concentration of pyrolysis gases lies in the neighbourhood of 350°C [43]. Systems of macropores almost spherical in shape with sporadic appearance and about hundreds of nm in radius were observed by SEM (Figure 6). The systems of mesopores concur in the neighborhood of these macropores.

Examples of the measured adsorption and desorption isotherms of CO_2 at a temperature of 25°C for resite (PF 150) and pyrolyzed samples (PF 800 and PF 1000) are given in Figure 7. These isotherms comply with their interpretation in Dubinin coordinates, with a correlation coefficient better than 0.999. Sample PF 800 shows a full overlap of the two sorption branches, and thus also the adsorption reversibility characteristic for physical adsorption. Other samples (PF 500, PF 600 and PF 700) showed the same behaviour. In the case of resite (PF 150), there is pronounced hysteresis of the desorption branch, connected with the fact that resite does not have a typical microporous system. In addition to adsorption, there is also absorption of CO_2 molecules between the chains of a three-dimensional polymer system [44]. The behaviour of adsorption-desorption isotherms differs from the behaviour of other pyrolyzed samples, see Figure 7,

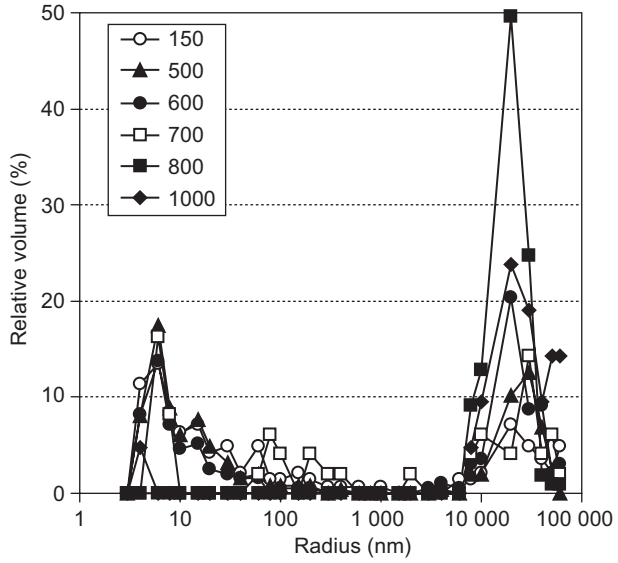

Figure 4. Distribution of meso-, macro- and coarse pores according to Hg porosimetry.

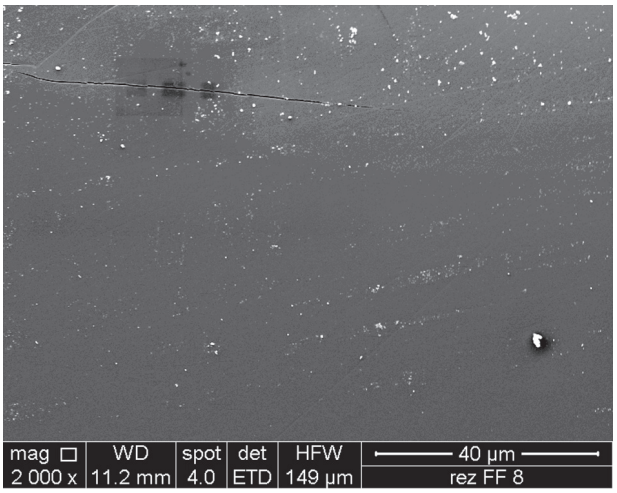

Figure 5. SEM image of a crack on the surface of sample PF 800.

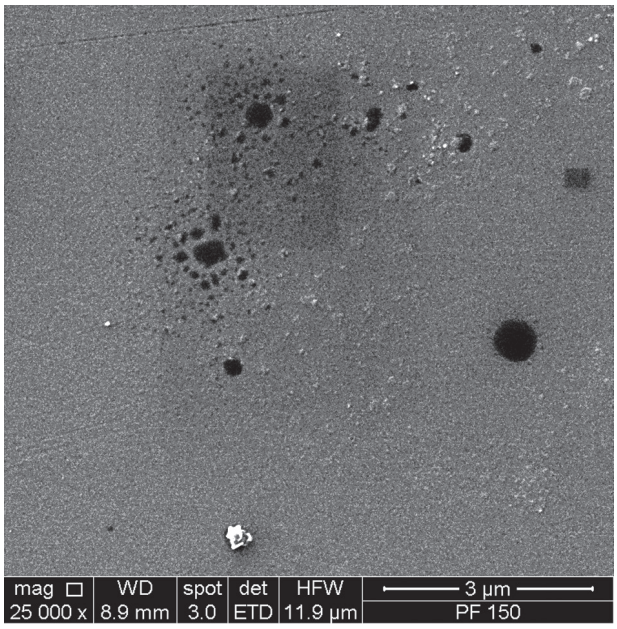

Figure 6. SEM image of meso- and macropores observed on the plane of the transversal section of the resite (PF 150) plane.

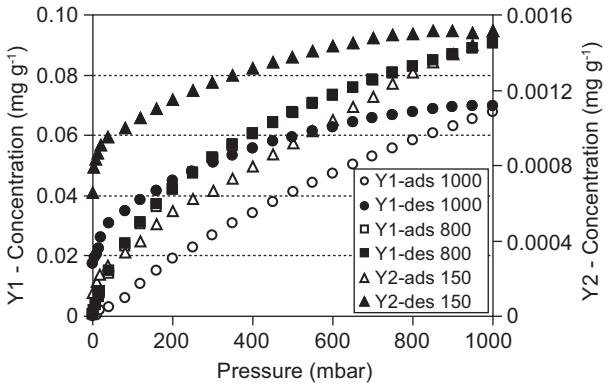

Figure 7. Comparison of CO_2 adsorption and desorption isotherms at 25°C.

indicating the different sorption properties of resite [11]. The same abnormality can be observed for the sample pyrolyzed at 1000°C which, unlike sample PF 150, has high microporosity. The hysteresis of the adsorption and desorption branch of the isotherm probably indicates chemisorption, which can appear similarly to absorption in the isotherm. As has been discussed above, Raman spectroscopy shows that the amount of disordered polymeric carbon grows with increasing pyrolysis temperature. This material may still contain significant amounts of oxygen and other impurities, as it has been proved by Evelyn et al. [41], which can potentially react with the sorbed gas. Another possibility is that the structure of the disordered polymeric carbon imitates the structure of the three-dimensional system of resite.

Mechanical properties

The results of measurements of the three- and four-point bending strength at laboratory temperature are shown in Figure 8. The ultimate strength in bending for phenol-formaldehyde resite and pyrolyzates has been measured by several researchers [28,29,45], but only in a three-point arrangement. This configuration can be questionable for measuring brittle materials. The stress for three-point bending varies from zero at the support points to a maximum at the centre of the sample. Thus only a very small portion of the specimen is subjected to a stress at or near the maximum value. However, in a four-point bending test, a larger part of the material is submitted to the maximum bending stress and, consequently, to a higher probability of crack propagation (based on probability of higher amount of occasional distributed failures). The results obtained by this test are therefore more realistic and more objective. For this reason, four-point bending rather than three-point bending is often preferred, and is widely used in tests on fragile materials or ceramics to obtain design data [46]. Figure 8 shows that, e.g. for values at 1000°C for three-point bending strength, the confidence interval is 89.4-195.5 MPa, while in the case of four-point bending strength the confidence interval is 113.9-132.5 MPa (both at confidence level 0.05, n = 6). It follows from these values that a four-point bending test can be better evaluated statistically. Four-point bending strength increased slightly with HTT in the temperature range 500-1000°C. In this temperature range, the structures of pyrolyzates contain mainly micropores, which do not influence the bending strength. The minimum value at 500°C is due to dramatic changes in the resin structure. Maximum values are reached at 1000°C. The slight decrease in strength at 800°C may be caused by the occasional occurrence of a surface crack, as was observed by SEM (Figure 5). The resite sample embodies relatively high four-point bending strength comparable to sample PF 700. The texture of the resite sample consists mainly of mesopores and occasional macropores nearly spherical in shape, observed by SEM (Figure 6), which do not have a negative influence on the strength and fracture toughness. In order to obtain a more objective understanding of the material fracture behaviour, bending tests were supplemented by fracture toughness measurements.

Both resonant and static Young's moduli (Figure 9) reached their minimum values at 500°C. Almost the same values were measured for the resite sample (PF 150). A remarkable increase in the moduli takes place at temperatures higher than 500°C. A maximum value exceeding 30 GPa was observed at 1000°C. E_{res} and E_{stat} in the temperature range 600-1000°C differ only insignificantly, which is in agreement with the glassy nature of glassy carbon, in which no visco-elastic effects can take place [45]. The differences between the static and resonant measurement values for PF 150 can be explained by the visco-elastic behaviour of the studied materials. This behaviour cannot be excluded at 500°C. All values displayed statistically significant differences (Mann-Whitney post-hoc test, α = 0.05). As shown in Figures 8 and 9, the ultimate strength in bending is much

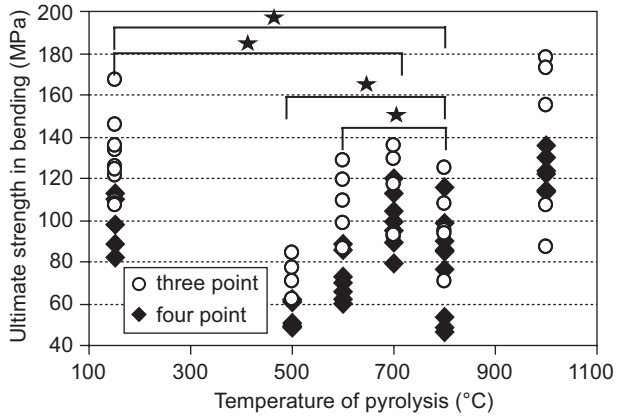

Figure 8. Variation in ultimate strength in bending with temperature of pyrolysis; ★ denotes values without statistically significant differences (four-point bending test, Mann-Whitney post hoc test, α = 0.05).

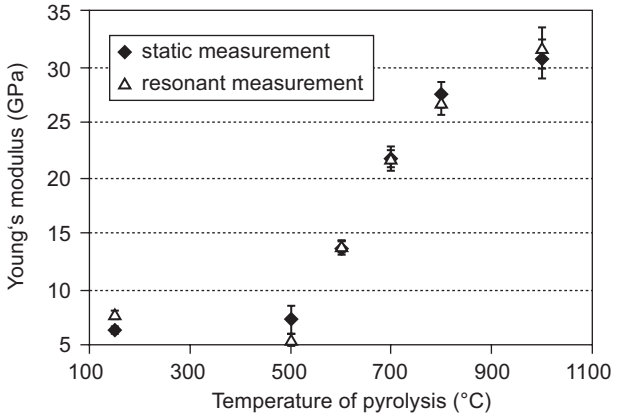

Figure 9. Variation in Young's moduli with temperature of pyrolysis; all values displayed statistically significant differences (Mann-Whitney post-hoc test, α = 0.05).

more sensitive than the modulus to structural faults.

The fracture resistance represented by fracture toughness K_{IC} is shown in Figure 10. The fracture toughness was measured using the chevron notch technique. The resite sample exhibits significantly higher fracture toughness values than the other samples. The fracture toughness of the cured material is relatively high at a level of 1.87 MPa $m^{0.5}$. Microstructural changes that take place during pyrolysis at 500°C cause a rapid decrease in fracture toughness to a measured minimum mean value of 0.46 MPa $m^{0.5}$. Then, with increasing pyrolysis temperature the fracture toughness increased slightly to a value of 0.85 MPa $m^{0.5}$, which was reached at 1000°C.

Microstructural changes take place during the change of condition of a material from the organic stage to the predominantly carbonaceous stage. This is demonstrated in Figure 11, which shows representative fracture surfaces of broken fracture toughness samples. The fracture surface of the sample prepared at 150°C (Figure 11a) shows a fracture pattern typical for brittle polymers, which are relatively rough. This explains the higher fracture toughness values. The sample prepared at 500°C shown in Figure 11b has a glassy-like fracture surface, suggesting low fracture resistance. The fully pyrolyzed material exhibits some toughening effects due to the presence of pores (developed during pyrolysis), as shown in Figure 11c.

Loading curves (load-indentation depth traces) were obtained by applying 1.96 N or 4.9 N using Vickers indenters HV02 and HV05. The natural behaviour of the material makes it impossible to measure the Vickers hardness values from the indenter imprints, so only the Martens hardness (determined from the indentation

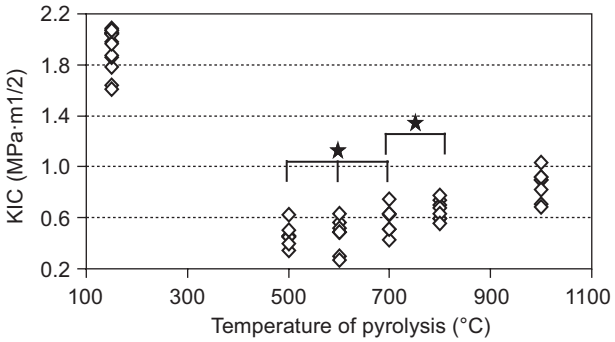

Figure 10. Variation in fracture toughness (KIC) with temperature of pyrolysis; ★ denotes values without statistically significant differences (Mann-Whitney post-hoc test, α = 0.05).

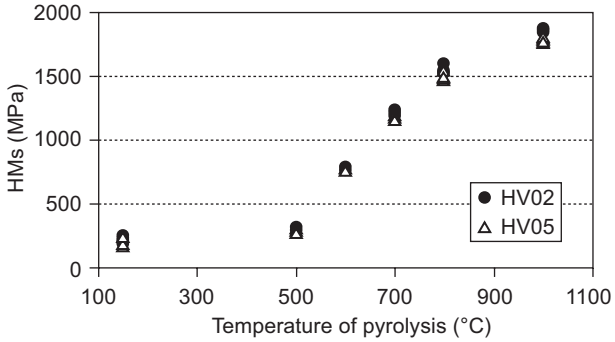

Figure 12. Variation of Martens hardness (HMs) with temperature of pyrolysis, all values displayed statistically significant differences (Mann-Whitney post-hoc test, α = 0.05).

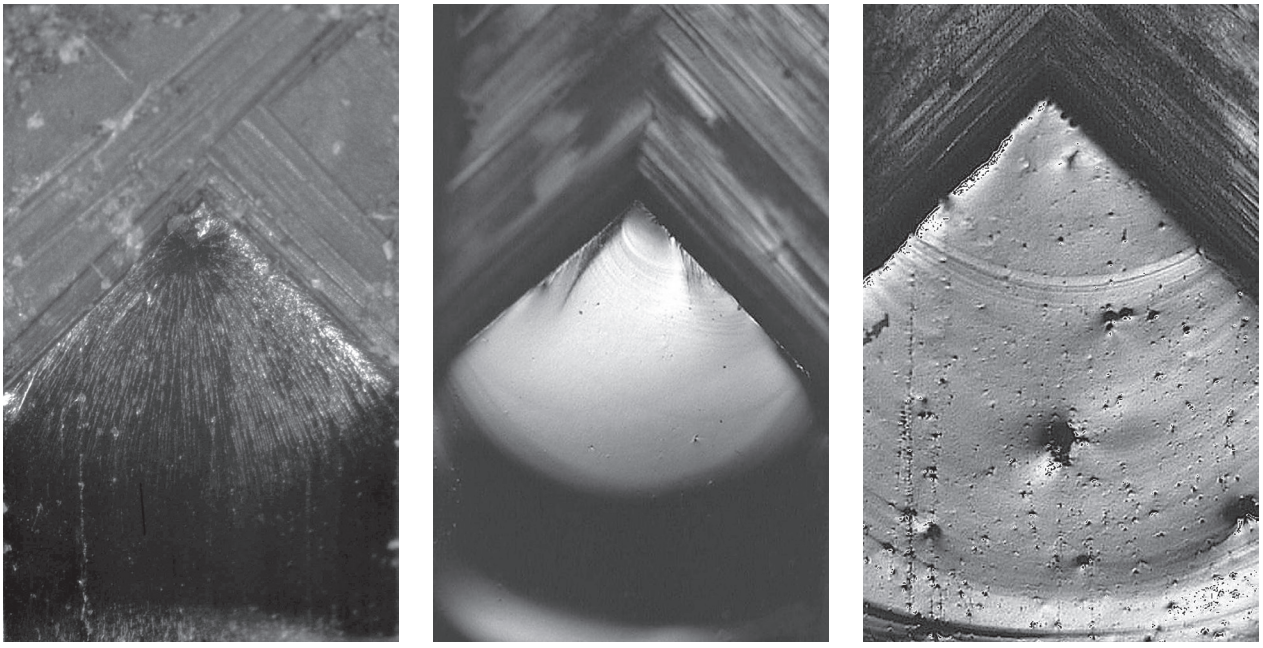

a) 150°C b) 500°C c) 1000°C

Figure 11. Typical fracture surfaces from the broken fracture toughness samples for temperature of pyrolysis 150, 500 and 1000°C.

depth) was measured. Figure 12 summarizes the results obtained for load levels 1.96 N and 4.9 N. The trend is clearly similar as for the measured Young's moduli (see Figure 9). The higher load led to slightly lower hardness values for the fully pyrolyzed samples.

CONCLUSIONS

A study has been made of the relation between the pyrolysis temperature of phenol formaldehyde resin, the development of a porous structure, and the mechanical properties. This problem has not previously been studied in its entirety.

The most dramatic changes in phenol formaldehyde resin structure occur in the 500-600°C range. This fact becomes evident by changes in bulk density, porosity and mechanical properties. Phenol-formaldehyde resin shows an increasing trend in the porosity of the micropores in the temperature interval from 500 till 1000°C, together with closure of the mesopores and macropores. In the resite sample (PF 150), mesopores, which may serve for removing the pyrolysis gases, prevail over other pore types. The resite sample pronounced hysteresis of the desorption branch due to absorption of CO_2 molecules between the chains of a three-dimensional polymer system. The same abnormality was observed for a sample pyrolyzed at 1000°C, and probably indicates chemisorption. It was proved by Raman spectroscopy that with increasing pyrolysis temperature, the amount of disordered polymeric carbon grows. Impurities, e.g. oxygen, can potentially react with the sorbed gas. Another possibility is that the structure of disordered polymeric carbon imitates the structure of the three-dimensional system of resite.

The ultimate bending strength was measured by four-point arrangement that is more suitable for measurement of brittle materials. The chevron notch technique was used for determining the fracture toughness. Observed three-dimensional surface changes after fracture toughness test were used to gain information about possible damage or development of cracks in prepared materials.

The results for the mechanical properties indicated that phenol-formaldehyde resin pyrolyzates behave similarly to ceramic materials. In the temperature range 500–1000°C, the strength, hardness and Young's modulus increased as the material became more brittle. Only the occasional occurrence of coarse pores in the form of cracks can influence the strength of the materials. By contrast, micropores and macropores almost spherical in shape had no negative influence on the mechanical properties.

The optimal carbonization temperature appears temperature interval 700 – 800°C. At these temperatures, the structure of phenol-formaldehyde resin is already in stable condition. Values of mechanical properties are slightly lower compared to material pyrolyzed at 1000°C. However this material showed the hysteresis of the adsorption and desorption branch of the isotherm which can negatively affect the separative function of membrane. Indispensable factor are economics of preparation owing to high energy requirement.

Our data on the material can be used for calculating the technical design of gas separation membranes.

Acknowledgement

The authors wish to acknowledge the financial support provided for GACR project 203/09/1327 by the Czech Science Foundation.

References

1. Pandey P., Chauhan R.S.: Progr. Polym. Sci. *26*, 853 (2001).
2. Zhang X., Hu H., Zhu Y., Zhu S.: J. Membr. Sci. *289*, 86 (2007).
3. Lagorsse S., Magalhães F.D., Mendes A.: J. Membr. Sci. *241*, 275 (2004).
4. Ismail A.F., David L.I.B.: J. Membr. Sci. *193*, 1 (2001).
5. Kolář F., Balík K., Yamada Y, Svítilová J., Mareček M.: Acta Montana B *10* (117), 91 (2000).
6. Kolář F., Svítilová J.: Ceramics-Silikaty *40*, 67 (1996).
7. *International Union of Pure and Applied Chemistry (IUPAC) Manuals of Symbols and Terminology for Physico Chemical Quantities and Units;* Butterworth: London, U.K. 1972.
8. Morterra C., Low M.J.D.: Carbon *23*, 525 (1985).
9. Ouchi K., Honda H.: Fuel *38*, 429 (1959).
10. Křístková M., Weiss Z., Filip P., Peter R.: Polym. Degrad. Stabil. *84*, 49 (2004).
11. Fott P., Kolář F., Weishauptová Z.: Acta Montana B *3* (91) 5 (1994).
12. Miura K., Hayashi J., Hashimoto K.: Carbon *29*, 653 (1991).
13. Fitzer E., Schaefer W., Yamada S.: Carbon *7*, 643 (1969).
14. Centeno T.A., Fuertes A.B.: J. Membr. Sci. *160*, 201 (1999).
15. Kim M.I., Yun C.H., Kim Y.J., Park C.R., Inagaki M.: Carbon *40*, 2003 (2002).
16. Lenghaus K., Qiao G.G., Solomon D.H., Gomez C., Rodriguez-Reinoso F., Sepulveda-Escribano A.: Carbon *40*, 743 (2002).
17. Kyotani T.: Carbon *38*, 269 (2000).
18. Inagaki M.: New Carbon Mater. *24*, 193 (2009).
19. Nishiyama N., Zheng T., Yamane Y., Egashira Y., Ueyama K.: Carbon *43*, 269 (2005).
20. Malshe V.C, Sujatha E.S.: React. Funct. Polym. *43*, 183 (2000).
21. Zhai D., Du H., Li B., Zhu Y., Kang F.: Carbon *49*, 725 (2011).
22. Zhang X., Hu H., Zhu Y., Zhu S.: J. Membr. Sci. *289*, 86 (2007).
23. Xu S., Li J., Qiao G., Wang H., Lu T.: Carbon *47*, 2103 (2009).
24. Moreira R.F.P.M., José H.J., Rodrigues A.E.: Carbon *39*, 2269 (2001).
25. Huang M., Teng H.: Carbon *40*, 955 (2002).
26. Wang A., Kang F., Huang Z., et al.: Carbon *45*, 2323 (2007).

27. Gasrsuch A., Klepel O.: Carbon *43*, 2330 (2005).
28. Laušević Z., Marinković S.: Carbon *24*, 575 (1986).
29. Choe C.R., Lee K.H.: Carbon *30*, 247 (1992).
30. Glogar P., Balík K.: Acta Montana B *3* (91) 49 (1994).
31. Senturia S.D and Sheppard, Jr. N.F.: Adv. Polym. Sci. *80*, 1 (1986).
32. Washburn EW.: Phys. Rev. *17,* 273 (1921).
33. Bluhm J.I.: Eng. Fract. Mech. *7* (3) 93 (1975).
34. *Instrumented indentation test for hardness and material parameters*, ISO 14577, ISO, Geneva, Switzerland, 2001.
35. Dlouhý I., Chlup Z., Boccaccini D.N., Atiq S., Boccaccini A.R.: Composite A *34*, 1177 (2003).
36. Boccaccini A.R., Rawlings R.D., Dlouhý I.: Mater. Sci. Eng. A-Struct. Mater. Prop. Microstruct. Process. *347*, 102 (2003).
37. Costa L., Rossi di Montelera L., Camino G., Weil E.D., Pearle E.M: Polym.Degrad. Stabil. *56*, 23 (1997).
38. Conley R.T., Guadiana R.A.: *Thermal Stability of Polymers*, Marcel Dekker, Inc., New York 1970.
39. Saunders K.J.: *Organic Polymer Chemistry*, Chapman and Hall, London 1973.
40. Trick K.A. Saliba T.E.: Carbon *33*, 1509 (1995).
41. Evelyn A.L., Ila D., Jenkins G.M.: Nucl. Instrum. Methods Phys. Res. Sect. B *85*, 861 (1994).
42. Kishore N., Sachan S., Rai K.N., Kumar A.: Carbon *41*, 2961 (2003).
43. Kolář F., Fott P., Balík K.: Acta Montana B *3* (91) 23 (1994).
44. Medek J., Weishauptová Z., Kovář L.: Microporous Mesoporous Mat. *89*, 276 (2006).
45. Glogar P., Balík K., Kolář F., Marek J.: Acta Montana B *1* (85), 83 (1992).
46. Wachtman J.B., Roger Cannon W., John Matthewson M.: *Mechanical properties of ceramics*, 2nd ed. John Wiley and Sons. Inc., San Francisco, 2009.